# Influence of magnetic interactions on the magnetic properties of dilute AuMn alloys*

J. C. Liu, B. W. Kasell, and F. W. Smith
*Department of Physics, The City College of the City University of New York, New York, New York 10031*
(Received 24 October 1974)

We have measured the initial susceptibility $\chi$ and magnetization $M$ up to $H = 50$ kG of a series of AuMn alloys ($n$ = 50–2000-ppm Mn) from 1.2 to about 100 K. Our results for $\chi$ and $M$ obey quite well the scaling laws predicted for magnetic impurities which interact via the Ruderman-Kittel-Kasuya-Yosida (RKKY) interaction, viz., $\chi(n,T) = F_1(T/n)$ and $M(n,T,H)/n = F_2(T/n,H/n)$. From the observed decrease of the magnetization per impurity atom as the Mn concentration increases, $V_0 = (2.4 \pm 0.3) \times 10^{-37}$ erg cm$^3$ is determined for the strength of the RKKY interaction, $V(r) = (V_0 \cos 2k_F r)/r^3$. The observed approach to saturation of $M$ is also consistent with this value for $V_0$. For the spin per Mn atom we find $S = 2.25 \pm 0.1$, assuming $g = 2$.

## I. INTRODUCTION

When magnetic impurities are dissolved in nonmagnetic metals, the interaction between the conduction electrons and the localized magnetic moments of the impurities gives rise to a variety of interesting concentration- and temperature-dependent effects, which are observable experimentally in the thermal, magnetic, and transport properties of the alloy.[1] Of primary importance to this problem is the $s$-$d$ interaction, $-J\vec{S}\cdot\vec{\sigma}$, where $J$ is the exchange integral, $\vec{S}$ is the localized spin, and $\vec{\sigma}$ is the conduction-electron spin. The $s$-$d$ interaction is responsible for both single-impurity (Kondo) effects[1] and for the effects due to indirect impurity-impurity interactions via the Ruderman-Kittel-Kasuya-Yosida (RKKY) potential.[2] The characteristic energy for single-impurity effects is $k_B T_K$, where $T_K$ is the Kondo temperature, while for impurity-impurity effects the characteristic energy is $nV_0$, where $n$ is the concentration of magnetic impurities and $V_0$ is the strength of the RKKY interaction, $V(r) = (V_0 \cos 2k_F r)/r^3$.

If $k_B T_K > nV_0$, single-impurity effects dominate, if $k_B T_K < nV_0$, impurity-impurity interactions dominate, and if $k_B T_K \sim nV_0$, both interactions influence the experimental behavior. It is clearly of great interest to determine $T_K$ and $V_0$ for a given alloy system. The goals of this investigation are to determine $V_0$ for the AuMn-alloy system and to investigate the extent to which single-impurity (Kondo) effects are observable in the magnetic properties of AuMn alloys.

At very low concentrations $n$ when the magnetic impurities act independently of one another, theory predicts that experimentally observed quantities, such as magnetization and magnetic susceptibility, will be universal functions of $T/T_K$. At higher concentrations $n$ when the RKKY interactions between impurities dominate the behavior of the alloy, theory predicts that universal scaling laws will be obeyed,[3,4] with scaling parameter, which in this case is $n$ (as opposed to $T_K$), with the result that $\chi = F_1(T/n)$ and $M/n = F_2(T/n, H/n)$. For free spins it should be pointed out that a Brillouin function describes the magnetization: $M/n \propto B_S(H/T)$.

At high $T$ (such that $k_B T \gg nV_0$) Larkin *et al.*[5] have used a virial expansion of the free energy in a power series of the concentration of impurities $n$ to investigate the effect of the RKKY potential on the thermodynamic functions of dilute magnetic alloys. They predict for $k_B T \gg nV_0$ that

$$\chi = ng^2 \mu_B^2 S(S+1)/3(k_B T + \theta_S),$$

where $\theta_S = C_S nV_0$ and $C_S$ is a constant of order unity. In addition, in a magnetic field such that $g\mu_B H$ is much greater than both $k_B T$ and $nV_0$, they predict for the approach to saturation of the magnetization

$$M = g\mu_B Sn[1 - 2(2S+1)nV_0/3g\mu_B H]. \quad (1)$$

At very low temperatures or very high concentrations ($k_B T \ll nV_0$), a dilute magnetic alloy enters the spin-glass regime,[6] where the impurity spins are strongly correlated with each other but without long-range magnetic order present. Klein[7] has predicted the limiting low-$T$ behavior of a dilute magnetic alloy by considering a random molecular field $H$ that has a probability distribution function $P(H) = \Delta/\pi(\Delta^2 + H^2)$, where $\Delta$ is the width of $P(H)$. At $T = 0$ it is predicted[8] that the susceptibility is

$$\chi = 2ng^2 S(S+1)\mu_B/3\pi\Delta.$$

## II. EXPERIMENT

Magnetization measurements from 0 to 50 kG and from 1.2 to about 100 K have been made on a series of AuMn alloys (54, 105, 216, 521, 1005, 2110 ppm Mn). The samples were prepared by melting the constituents (Asarco 99.999% Au and Johnson Matthey 99.99% Mn) under an argon at-

TABLE I. Mn concentrations of AuMn alloys studied.

| $n_0$ (ppm Mn-nominal) | $n_1$ [a] (ppm Mn) | $n_2$ [b] (ppm Mn) | $n$ [c] (ppm Mn) |
|---|---|---|---|
| 50 | 50 | 58 | 54±4 |
| 100 | 97 | 113 | 105±8 |
| 200 | 225 | 207 | 216±9 |
| 500 | 557 | 485 | 521±36 |
| 1000 | 1030 | 980 | 1005±25 |
| 2000 | 2060 | 2160 | 2110±50 |

[a]Concentrations determined from residual resistance ratios $\rho$ and $n_1$ (ppm Mn) $= 8.81\times10^3\ \rho$ (see text).

[b]Concentrations determined from measured values of the Curie constant $C$ and saturation magnetization $M_{sat}$, listed in Table II, using $n_2 = M_{sat}^2/(3k_BC - g\mu_B M_{sat})$.

[c]Concentrations determined by averaging the values of $n_1$ and $n_2$ from this table, and used in the analysis of the data.

mosphere in an arc furnace. The polycrystalline samples, whose masses were 1-2 g, were annealed under vacuum for 24 h at 900 °C prior to measurement.

The Mn concentrations in the samples were determined both from measurements of the residual resistance ratios

$$\rho = \frac{R(4.2)}{R(273) - R(4.2)}$$

and the magnetic properties of the samples. In Table I we list the nominal concentrations $n_0$ for these samples, along with concentrations $n_1$ and $n_2$ determined as follows. $n_1$ is found from the measured values of $\rho$, using $n_1 = 8.81\times10^3\rho$. The constant $8.81\times10^3$ has been determined using the results of this work and those of Loram, Whall, and Ford.[9] $n_2$ is determined from measured values of the Curie constant $C = n_2 g^2 \mu_B^2 S(S+1)/3k_B$ and the saturation magnetization $M_{sat} = n_2 g\mu_B S$. Eliminating the spin $S$ and solving for $n_2$, we have

$$n_2 = M_{sat}^2/(3k_BC - g\mu_B M_{sat}).$$

Throughout this work we have assumed $g = 2$ for Mn impurities in Au.[10] The values of $C$ and $M_{sat}$ measured for these samples and used in determining $n_2$ are listed in Table II.

The Mn concentrations that we have chosen to use in the analysis of our data are listed in the last column of Table I and are the result of averaging $n_1$ and $n_2$. It should be noted that the values of $n$ so found are higher (by 0.5–8%) than the nominal concentrations $n_0$.

The magnetization has been measured by the Faraday method using a Cahn RH electrobalance (resolution 2 $\mu$g) and a Westinghouse superconducting solenoid (0–50 kG). Details of the experimental apparatus appear elsewhere.[11] Thermometry was provided from 1.2 up to 20 K by a calibrated Allen Bradley carbon resistor, while from 20 to 125 K a platinum resistance thermometer was used. These thermometers were calibrated against the susceptibility of chrome potassium alum.

Magnetization curves for these alloys were obtained by plotting the off-balance signal of the Cahn RH electrobalance as a function of applied magnetic field on an $X$-$Y$ recorder. For all the samples, the magnetization was corrected for the contribution from the diamagnetic susceptibility of pure Au, which was assumed to be $(-0.1435)\times10^{-6}$ emu/g.[12]

## III. RESULTS AND DISCUSSION

### A. Magnetic susceptibility

The magnetic susceptibility $\chi$, determined graphically from the slope of $M$ vs $H$ as $H \to 0$, has

TABLE II. Magnetic properties of AuMn alloys studied.

| $n$ (ppm Mn) | $C$ [a] ($10^{-6}$ emu K/g) | $\Theta$ [a] (K) | $M_{sat}$ [b] ($10^{-3}$ emu G/g) | $S$ [c] | $S$ [d] |
|---|---|---|---|---|---|
| 54 | 0.985±0.02 | 0 | 7.0±0.2 | 2.23±0.04 | 2.29±0.06 |
| 105 | 1.92±0.04 | 0 | 13.7±0.2 | 2.23±0.04 | 2.30±0.04 |
| 216 | 3.81±0.08 | 0 | 26.3±0.2 | 2.18±0.04 | 2.15±0.03 |
| 521 | 9.80±0.2 | +0.2±0.1 | 65±1 | 2.27±0.04 | 2.20±0.04 |
| 1005 | 20.2±0.4 | +0.02±0.1 | 133±3 | 2.34±0.04 | 2.33±0.04 |
| 2110 | 38.0±0.8 | −0.5±0.2 | 267±5 | 2.21±0.04 | 2.23±0.04 |

[a]Measured Curie constant $C$ and Curie-Weiss temperature $\Theta$ determined from initial susceptibility data and $\chi = C/(T+\Theta)$.

[b]Measured saturation magnetization $M_{sat}$ determined from magnetization data in the limit $1/H \to 0$ (see Fig. 5 and text).

[c]Values of the spin $S$ per Mn atom determined from the measured Curie constants $C = ng^2\mu_B^2 S(S+1)/3k_B$, $g=2$, and the concentrations $n$ listed in this table.

[d]Values of the spin $S$ per Mn atom determined from the measured saturation magnetizations $M_{sat} = ng\mu_B S$, $g=2$, and the concentrations $n$ listed in this table.

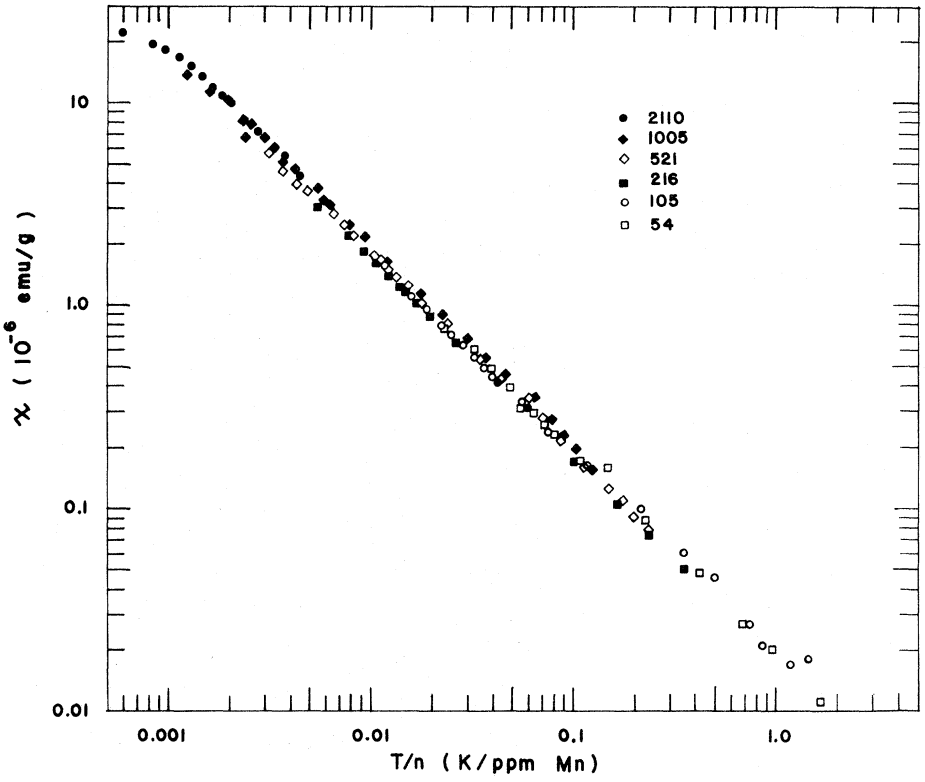


FIG. 1. Magnetic susceptibility $\chi(H \to 0)$ for six AuMn alloys (54, 105, 216, 521, 1005, 2110 ppm Mn) as a function of "reduced temperature" $T/n$. For clarity, overlapping data points have been omitted.

been measured from 1.2 up to about 100 K for the six AuMn alloys studied. The results for $\chi(T)$ for each alloy have been fitted to a Curie-Weiss law, $\chi(T) = C/(T+\Theta)$, with the resulting values of $C$ and $\Theta$ given in Table II. The only significant deviations from Curie-Weiss behavior occur below 2 K for $n$ = 1005 ppm Mn and below 4 K for $n$ = 2110 ppm Mn. These deviations are due to the "freezing-in" of the orientations of the Mn spins in the local molecular field. In Fig. 1 $\chi(n, T)$ is plotted as a function of $T/n$ to test the scaling prediction[4] $\chi(n, T) = F_1(T/n)$. The susceptibility data for the six alloys fall quite well on a universal curve, to within experimental error. Deviations from scaling at high or low concentrations such as previously observed in a similar plot for ZnMn[13] are not in evidence for these AuMn alloys.

From the measured Curie constants $C$ and concentrations $n$ listed in Table II we have calculated values for the impurity spin $S$, assuming[10] $g = 2$. The values of $S$ so obtained (Table II) are essentially independent of Mn concentration, yielding a spin $S = 2.25 \pm 0.1$. Also listed in Table II are spins $S$ obtained from the concentrations $n$ and saturation magnetizations $M_{sat}$, again assuming $g = 2$. We obtain $S = 2.25 \pm 0.1$, in excellent agreement with the average value obtained here from the low-field data. Previous susceptibility measurements[12] on AuMn have yielded $S = 2.37$, while saturation magnetization results[14] yield $S = 2.25$, in agreement with this work.

### B. Magnetization

In Fig. 2 the impurity magnetization at three different temperatures $T$ is plotted as a function of $H/T$ for the 54, 521, and 2110-ppm-Mn samples. Also shown on the graphs are Brillouin functions for for the appropriate Mn spin $S$, taken to be 2.29, 2.20, and 2.23 for these three samples, respectively (see the last column of Table II). For the 54-ppm-Mn sample, to within experimental error, the magnetization data are a function only of $H/T$ for these values of $H$ and $T$. The same behavior is found for the 105- and 216-ppm-Mn samples, not shown. In addition, for these three samples the experimental values for $M$ fall only slightly (1–5%) below the appropriate Brillouin function. The difference is measurable, however, and will be used to obtain $V_0$, the strength of the RKKY interaction.

For the 521-ppm-Mn sample $M$ is no longer a function of $H/T$ alone and deviations from the Brillouin function are significant. This behavior is more pronounced for the 1005-ppm-Mn sample, not shown, and is most evident for the 2110-ppm-Mn sample, as can be seen from Fig. 2. This behavior of the impurity magnetization with increasing $n$ has previously been observed for a series of ZnMn alloys where impurity-impurity interactions

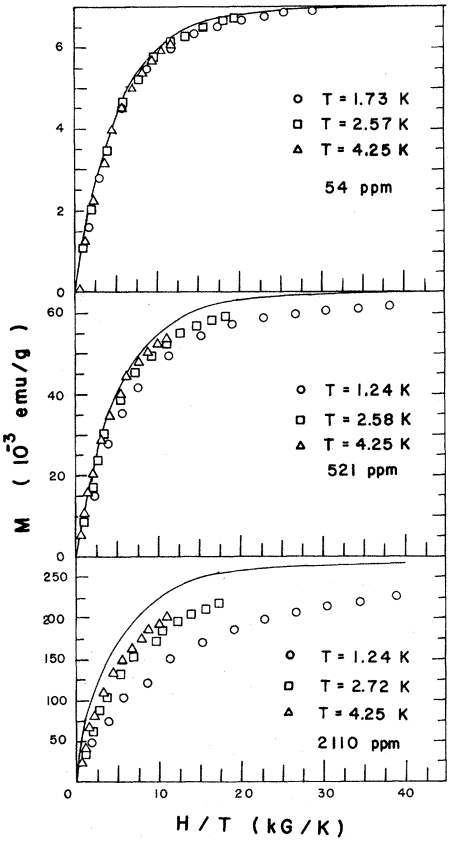


FIG. 2. Impurity magnetization $M$ as a function of $H/T$ for three AuMn alloys (54, 521, and 2110 ppm Mn), for several temperatures $T$ and for $H$ up to 47.45 kG. Also shown as the solid curves are the free-spin Brillouin functions $B_S(H/T)$, calculated using the spins $S$ listed in the last column of Table II for the appropriate alloy concentrations.

have been shown to be important.[13]

To test the scaling behavior of the magnetization,[4] in Fig. 3 we plot $M/M_{sat} = M/g\mu_B Sn$ as a function of $H/n$ for three alloys at fixed $T/n = (3.73 \pm 0.01) \times 10^{-3}$ K/(ppm Mn). The data superpose quite well on a single curve. There are no deviations from scaling observed for the 2110-ppm-Mn sample such as were previously observed for a similar concentration ZnMn sample.[13] Good agreement with scaling predictions for $M$ has also been observed for the three lower-concentration AuMn samples studied here, at higher values of $T/n$.

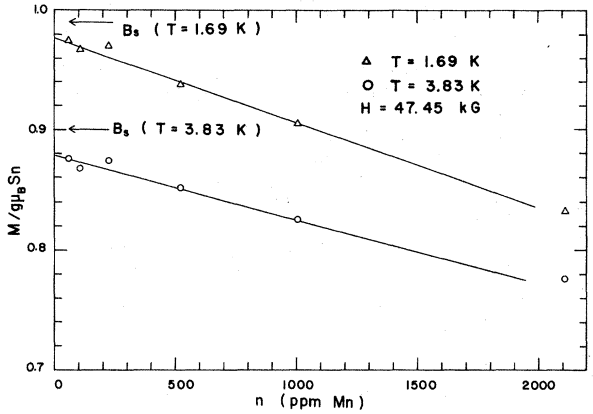


FIG. 4. Impurity magnetization $M$, normalized to $g\mu_B Sn = M_{sat}$, as a function of Mn concentration $n$ in a magnetic field $H = 47.45$ kG and at $T = 1.69$ and 3.83 K. Also indicated are the values of the free-spin Brillouin functions $B_S(H/T)$ for $S = 2.25$ at the appropriate $H$ and $T$.

To obtain the strength $V_0$ of the RKKY potential we plot in Fig. 4 $M/M_{sat}$ as a function of $n$ for $T = (1.69 \pm 0.06)$ K and $(3.83 \pm 0.04)$ K in a field of 47.45 kG. The initial linear decrease in $m = M/M_{sat}$ as a function of $n$ yields $V_0$ since, according to Larkin[5] [Eq. (1)], $\Delta m/\Delta n = -BV_0/H$, where $B = 2(2S+1)/3g\mu_B$. From the slope at $T = 3.83$ K we obtain $V_0 = (2.1 \pm 0.3) \times 10^{-37}$ erg cm$^3$, while at

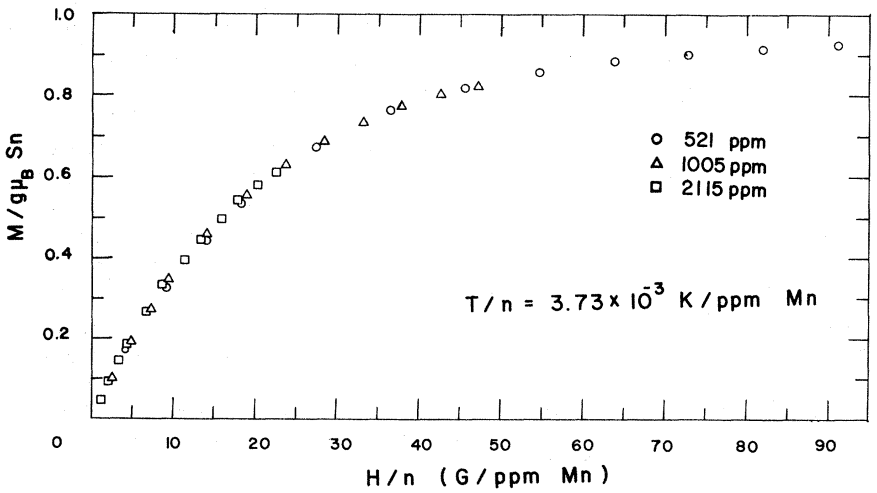


FIG. 3. Impurity magnetization $M$ divided by concentration $n$ (in ppm Mn) as a function of $H/n$ at the "reduced temperature" $T/n = (3.73 \pm 0.01) \times 10^{-3}$ K/(ppm Mn). For $n = 521$, 1005, 2110 ppm Mn, the corresponding temperatures are $T = 1.94$, 3.75, 7.90 K, respectively.

$T = 1.69$ K, $V_0 = (2.7 \pm 0.3) \times 10^{-37}$ erg cm$^3$ is obtained, in both cases using $S = 2.25$ and $g = 2$. The average value obtained is $V_0 = (2.4 \pm 0.3) \times 10^{-37}$ erg cm$^3$, which is an order of magnitude less than the value $V_0 = 2 \times 10^{-36}$ erg cm$^3$ found for ZnMn alloys.[13] We note that $V_0/k_B = (1.04 \pm 0.12)$ K/at. % Mn) for AuMn and that $V_0/k_B = (9.7$ K/at. %Mn) for ZnMn.. Also shown in Fig. 4 are values of (free-spin) Brillouin functions for $S = 2.25$ and the appropriate $T$ and $H$. The linear extrapolation of $M/M_{sat}$ to $n = 0$ falls about 1–2% below this free-spin prediction. For ZnMn a similar but much greater difference of about 10% was observed as $n \to 0$.[13] This further illustrates the relative weakness of the interaction between the conduction electrons and the Mn impurities in AuMn as compared to ZnMn.

An alternative method of obtaining $V_0$ from the magnetization data is to examine the saturation behavior of $M$. This is displayed in Fig. 5 where $M$ is plotted as a function of $H^{-1}$ for the 521-, 1005-, and 2110-ppm-Mn samples. The prediction of Larkin[5] [Eq. (1)] describes reasonably well the approach to saturation ($H^{-1} \to 0$) of $M$ for the 1005- and 2110-ppm-Mn samples. However, as observed also for ZnMn,[13] the slope of $M$ vs $H^{-1}$ is temperature dependent and $M$ can be represented by the following expression:

$$M = g\mu_B Sn[1 - H_0(n, T)/H], \qquad (2)$$

where $H_0(n, T) = Ak_B T + BnV_0$. By comparison with Eq. (1) we make the following identification: $B = 2(2S+1)/3g\mu_B$. In Fig. 6 we plot

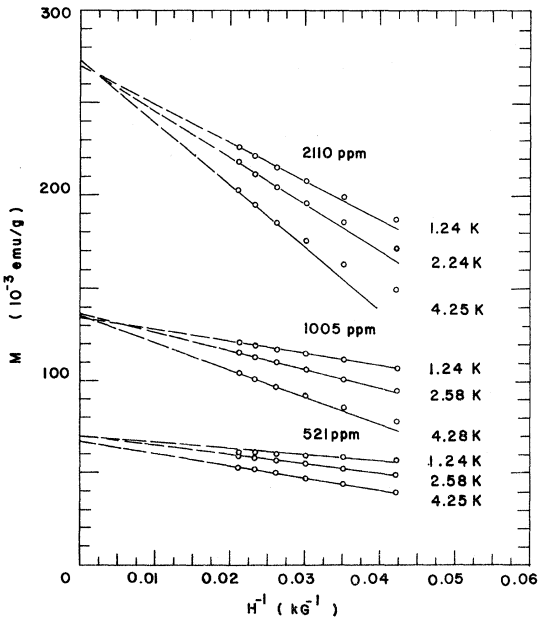


FIG. 5. Impurity magnetization $M$ for the 521-, 1005-, and 2110-ppm-Mn alloys as a function of the inverse of the magnetic field $1/H$ for several temperatures.

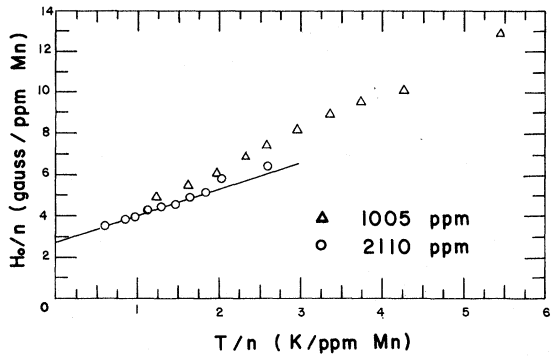


FIG. 6. $H_0(n, T)/n$ as a function of the "reduced temperature" $T/n$ for the 1005- and 2110-ppm-Mn alloys. The straight line indicates the fit to the equation $H_0/n = Ak_B T/n + BV_0$ for the 2110-ppm-Mn data. See Eq. (2) for the definition of $H_0$.

$$H_0(n, T)/n = Ak_B T/n + BV_0$$

as a function of $T/n$ for the 1005- and 2110-ppm-Mn alloys. The straight line drawn through the data points has an intercept at $T/n = 0$ equal to $BV_0$ and a slope equal to $Ak_B$. From the intercept of the straight line drawn in Fig. 6 we find $V_0 = (2.4 \pm 0.2) \times 10^{-37}$ erg cm$^3$, using $g = 2$ and $S = 2.25$ to determine $B$. This value for $V_0$ is identical with that found from the dependence of $M/M_{sat}$ on $n$. From the slope of the straight line we find $Ak_B = (1.23 \pm 0.2) \times 10^3$ G/K, compared to $2.9 \times 10^3$ G/K for ZnMn.[13] For the ratio of the coefficients appearing in $H_0$, we find $A/B = (0.045 \pm 0.01)$. We as yet have no explanation for this $Ak_B T$ term in $H_0$ except to say that it seems to represent a single-impurity contribution due either to free spins or to the Kondo effect.

The data plotted in Fig. 5 for the 521-ppm-Mn sample cannot be represented by Eq. (2) due to a more rapid approach to saturation than $H^{-1}$. The same is also true for the three lowest-concentration alloys. This approach to saturation more rapid than $H^{-1}$ is also characteristic of the Brillouin function for free spins. Hence it appears that for the 54-, 105-, 216-, and 521-ppm-Mn alloys, the approach to saturation of the magnetization is not completely dominated by impurity-impurity interactions via the RKKY potential. Instead, it appears that single-impurity effects also play a role. If we conclude that $nV_0$ and $k_B T_K$ are comparable energies in this concentration region, then, using $V_0 = 2.4 \times 10^{-37}$ erg cm$^3$ and $n = (300 \pm 200)$ ppm Mn, we obtain $T_K \sim (3 \pm 2) \times 10^{-2}$ K. This $T_K$ is of the same order of magnitude as the result obtained from nuclear orientation measurements in AuMn,[15] and would seem to preclude $T_K \sim 10^{-13}$ K as obtained from the analysis of resistivity data for AuMn.[9]

It is of interest at this point to further compare the two dilute alloy systems AuMn and ZnMn in terms of the relative strengths of the conduction-electron–magnetic-impurity interaction and its effect on the magnetic properties of the alloys. With $V_0 = 2\times10^{-36}$ erg cm$^3$, ZnMn is clearly a more strongly interacting system than AuMn with $V_0 = 2.4\times10^{-37}$ erg cm$^3$. This stronger coupling of the Mn impurity to the host conduction electrons is reflected in the smaller spin, $S\sim1.25$ for 100 ppm Mn in Zn[13] compared to $S\sim2.25$ for 100 ppm Mn in Au. The divalent Mn ion, $Mn^{2+}$, has a spin $S = \frac{5}{2}$ according to Hund's rules. In addition, the single-impurity (Kondo) effect in AuMn, with $T_K \sim 10^{-2}$ K, is weaker than in ZnMn, where $T_K \sim 0.28$ K.[16]

Even though $V_0$ for AuMn is smaller than in ZnMn, it appears that "ideal" spin-glass behavior extends over a wider concentration range in AuMn than in ZnMn. By "ideal" spin-glass behavior we mean that the behavior of the magnetic impurities is dominated by the RKKY interaction, with observed deviations from the RKKY scaling laws for experimental quantities being negligible. Owing to stronger conduction-electron–impurity interactions in ZnMn, significant deviations from RKKY scaling laws due to the single-impurity (Kondo) effect will extend to higher concentrations, $n\sim k_B T_K/V_0$, in ZnMn than in AuMn. This is due to the fact that $T_K$ increases more rapidly than $V_0$ as a function of the exchange integral $J$, viz., $T_K \propto e^{-1/N_0 J}$, while $V_0 \propto J^2$. Thus, as $J$ increases by about a factor of 3 from AuMn to ZnMn, $T_K$ increases by a factor of 20 while $V_0$ increases by about a factor of 9. Since for ZnMn $T_K \sim 0.28$ K, a value of $T_K$ for AuMn equal to about $10^{-2}$ K is reasonable.

At higher Mn concentrations deviations from RKKY scaling will again be seen, this time due to self-damping of the RKKY oscillations.[17] This is essentially a mean-free-path effect which gives rise to an exponential decay of the RKKY oscillations. The $1/r^3$ dependence of $V(r)$ will no longer be strictly correct, and hence the simple RKKY scaling laws for $\chi$ and $M$ will no longer be valid.[4] This self-damping effect may explain deviations from RKKY scaling seen for ZnMn at about 2000 ppm Mn.[13] No such deviations are seen in this work at 2000 ppm Mn in Au. The electronic mean free path decreases about six times faster per unit Mn concentration in dilute ZnMn alloys[18] than in dilute AuMn alloys.

## IV. CONCLUSIONS

We have determined the strength of the RKKY interaction in dilute AuMn alloys to be $V_0 = (2.4 \pm 0.3)\times10^{-37}$ erg cm$^3$. Assuming $g = 2$, the spin per Mn atom is found to be $S = 2.25 \pm 0.1$. For the AuMn alloys studied, with concentrations in the range 50–2000 ppm Mn, our results for $\chi$ and $M$ agree quite well with the RKKY scaling laws. From the approach to saturation of $M(H)$ and its dependence on Mn concentration for these alloys, we conclude that $T_K \sim 10^{-2}$ K for AuMn. This result receives further confirmation from a comparison with ZnMn alloys, where $T_K \sim 0.28$ K and $V_0 = 2\times10^{-36}$ erg cm$^3$.

We are extending our measurements of $V_0$ to the dilute alloy systems AgMn and CuMn to aid in our understanding of the RKKY interaction and the factors which determine its strength within different hosts.

## ACKNOWLEDGMENT

We wish to thank Professor M. P. Sarachik for valuable discussions.

*Research supported by the National Science Foundation, Grant No. GH-34672 and by CUNY FRAP Grant No. 10646.

[1]For reviews of both the theoretical and experimental sides of the Kondo effect see, *Magnetism*, edited by H. Suhl (Academic, New York, 1973), Vol. 5.

[2]M. A. Ruderman and C. Kittel, Phys. Rev. 96, 99 (1954); T. Kasuya, Progr. Theor. Phys. 16, 45 (1956); K. Yosida, Phys. Rev. 106, 893 (1957).

[3]A. Blandin, thesis (Paris University, 1961) (unpublished); A. Blandin and J. Friedel, J. Phys. Radium 20, 160 (1959).

[4]J. Souletie and R. Tournier, J. Low Temp. Phys. 1, 95 (1969).

[5]A. I. Larkin and D. E. Khmel'nitskii, Zh. Eksp. Teor. Fiz. 58, 1789 (1970) [Sov. Phys.–JETP 31, 958 (1970)]; A. I. Larkin, V. I. Mel'nikov, and D. E. Khmel'nitskii, Zh. Eksp. Teor. Fiz. 60, 846 (1971) [Sov. Phys.–JETP 33, 458 (1971)].

[6]For a good review of the theory of spin glasses see P. W. Anderson [in *Proceedings of the International Symposium on Amorphous Magnetism*, edited by H. O. Hooper and A. M. deGraff (Plenum, New York, 1973), p. 1].

[7]M. W. Klein and R. Brout, Phys. Rev. 132, 2412 (1963); M. W. Klein, Phys. Rev. 136, A1156 (1964); 173, 552 (1968).

[8]M. W. Klein and L. Shen, Phys. Rev. B 5, 1174 (1972).

[9]J. W. Loram, T. E. Whall, and P. J. Ford, Phys. Rev. B 3, 953 (1971).

[10]D. Shaltiel and J. H. Wernick, Phys. Rev. 136, A245 (1964).

[11]J. B. Haddad, Ph.D. thesis (City College of the City University of New York, 1974) (unpublished).

[12]C. M. Hurd, J. Phys. Chem. Solids 30, 539 (1969).

[13]F. W. Smith, Phys. Rev. B 10, 2980 (1974).

[14]B. Manhes, thesis (Grenoble, 1971) (unpublished).

[15]E. Lagendijk, L. Niesen, and W. J. Huiskamp, Phys. Lett. A 30, 326 (1969).

[16]F. W. Smith, Phys. Rev. B 10, 2034 (1974).

[17]A. J. Heeger, A. P. Klein, and P. Tu, Phys. Rev. Lett. 17, 803 (1966); R. E. Walstedt and L. R. Walker, Phys. Rev. B 9, 4857 (1974).

[18]F. W. Smith, Phys. Rev. B 9, 942 (1974).